Ontogeny of swimming movements in bronze corydoras (*Corydoras aeneus*)

Q. Mauguit, D. Olivier, N. Vandewalle, and P. Vandewalle

Abstract: Fish larvae experience fundamental morphological, physiological, and physical changes from hatching to adulthood. All of these changes have an effect on the locomotor movements observed in the larvae. We describe the development of swimming movements in larval bronze corydoras (*Corydoras aeneus* (Gill, 1858); Ostariophysi, Siluriformes) during their ontogeny. Swimming movements of adults and larvae, aged 0–512 h posthatching, were recorded at 500 frames/s. Movements were analyzed by digitizing points along the fish midline. Movements are described by direct (swimming speed and amplitude of landmarks) and indirect (r^2_{mean} and CV of r^2 as movement coordination indices; Strouhal number as an efficiency index) parameters. The increase in swimming speed correlated with improvement of movement coordination in both larvae and adults, as well as with an increase in swimming efficiency in larvae. Directly after hatching, swimming movements were coordinated but were not efficient. Efficiency increased rapidly with fish growth up to 8 mm total fish length and disappearance of the yolk sac. These events were coupled with reduction of the maximal lateral amplitude observed along the whole body during swimming. The anguilliform swimming mode was used at hatching, but a transition to the carangiform mode was observed at approximately 17 mm total fish length.

Résumé : De l'éclosion à l'âge adulte, les larves de poissons connaissent des changements morphologiques, physiologiques et physiques fondamentaux. Toutes ces modifications affectent les mouvements de locomotion observés chez les larves. Notre travail décrit le développement les mouvements de locomotion chez des larves de corydoras bronzés (*Corydoras aeneus* (Gill, 1858); Ostariophyses, Siluriformes) durant l'ontogenèse. Nous avons enregistré les mouvements de nage d'adultes et de larves âgées de 0 à 512 heures après l'éclosion à une fréquence de 500 images/s. Pour l'analyse, nous avons digitalisé des points le long de la ligne médiane des poissons. Nous avons décrit les mouvements à l'aide de variables directes (vitesse de nage et amplitude des points de repère) et indirectes ($r^2_{moyenne}$ et CV de r^2 comme indices de coordination du mouvement; nombre de Strouhal comme indice d'efficacité). Il existe une corrélation entre l'accroissement de la vitesse de nage et d'une part, l'amélioration de la coordination tant chez les larves que chez les adultes et d'autre part, l'augmentation de l'efficacité de la nage chez les larves. Tout juste après l'éclosion, les mouvements de nage sont coordonnés, mais non efficaces. L'efficacité augmente rapidement avec la croissance jusqu'à ce que les larves atteignent une taille de 8 mm et que le sac vitellin ait disparu. Ces événements coïncident avec la réduction de l'amplitude latérale maximale observée tout le long du corps durant la nage. Le mode de nage anguilliforme est utilisé à l'éclosion, mais il se produit une transition au mode carangiforme à une longueur totale d'environ 17 mm.

[Traduit par la Rédaction]

Introduction

Swimming movement ontogeny has been studied in various species, such as the cyprinids zebra danio (*Danio rerio* (Hamilton, 1822)) (Fuiman and Webb 1988; Müller and van Leeuwen 2004; Fontaine et al. 2008; Müller et al. 2008) and common carp (*Cyprinus carpio* L., 1758) (Osse 1989; Osse and van den Boogaart 1999, 2000), the pleuronectid European plaice (*Pleuronectes platessa* L., 1758) (Batty 1981, 1983), and the clupeid Atlantic herring (*Clupea harengus* L., 1758) (Batty 1984). To our knowledge, however, there exists no comparison between the swimming ontogenies of

two closely related species practicing two different swimming modes at adulthood. Moreover, the study of swimming ontogeny has often been limited to a few developmental stages generally occurring after complete absorption of the yolk sac.

Many fish generate backward-traveling waves of increasing amplitude along their bodies to propel themselves forward (Gray 1933). The propulsive wave is powered by the axial musculature and depends mainly on the material properties and shape of the body (Müller and van Leeuwen 2004). During swimming, the water opposes fish displacement with viscous and inertial forces (Sfakiotakis et al. 1999). The ratio of inertial to viscous fluid dynamic forces is expressed by the dimensionless Reynolds number: $Re = U \times TL \times \nu^{-1}$, where TL is the total fish length, U is the relative swimming speed, and ν the kinematic viscosity of the fluid. Because fish size plays a significant role in the flow regime, fish experience a gradual change of flow regime during growth. At hatching, larvae measure a few millimetres and the corresponding Re value ranges from 10 to 900, corresponding to an intermediate flow regime (Fuiman and Batty 1997; McHenry and Lauder 2005). Both

Q. Mauguit,[1] D. Olivier, and P. Vandewalle. Laboratoire de Morphologie Fonctionnelle et Evolutive, Université de Liège, B-4000 Liège, Belgium.
N. Vandewalle. GRASP, Institut de Physique, bâtiment B5a, Université de Liège, B-4000 Liège, Belgium.

[1]Corresponding author (e-mail: Q.Mauguit@ulg.ac.be).

viscous and inertial forces play important roles in locomotor behaviors. In adult fish, *Re* values are greater than 1 000 and can increase up to 100 000 (McHenry and Lauder 2005). When the flow regime is inertial, viscous forces are negligible.

Undulatory swimmers use different resistive or reactive mechanisms to produce forces in viscous compared with inertial flow regimes (Webb and Weihs 1986; Videler 1993). In the intermediate flow regime, thrust will be generated partly according to the resistive model and partly to the reactive model (Webb and Weihs 1986). According to the resistive model, larvae must move with large body wave amplitudes along their whole body to exploit the viscous force optimally (Weihs 1980; Batty 1981, 1984; Webb and Weihs 1986). This may explain why the larvae of fish such as the sharptooth catfish (*Clarias gariepinus* (Burchell, 1822)) (Mauguit et al. 2010) or *D. rerio* (Müller and van Leeuwen 2004) are known to use the anguilliform swimming mode in their first developmental stage. In the inertial flow regime, the reactive model prevails: fish need not move their entire bodies to generate thrust (Lauder and Tytell 2006). The carangiform swimming mode is well adapted to the inertial flow regime, as only the last posterior third of the body undulates (Weihs 1974). The anterior part of the body is used to generate propulsive forces that are transferred to the caudal peduncle and fin, which act as a discrete propeller (Videler 1993). Reduced body undulations also lead to decreased drag (Lighthill 1975).

Swimming ontogeny is not only influenced by physical factors; some biological factors also play a significant role. During growth, larvae lose existing systems (e.g., the yolk sac; Hale 1999; Müller and van Leeuwen 2004) and recruit new structures (e.g., various fins developing from fin folds; Weihs 1973; Osse and van den Boogaart 1995). The neural system develops (Carrier 1996), the notochord transforms into the vertebral column (Long et al. 1994; Carrier 1996; Long and Nipper 1996), and changes in muscle fiber type and in axial muscle morphology can occur (van Raamsdonk et al. 1978).

Studies of fish swimming ontogeny have been performed mostly with the same kinematic methods used for adult fish, but these methods are not perfectly suited for studying swimming movements throughout fish development. Consequently, Mauguit et al. (2010) developed a new method for describing more precisely the establishment of swimming movements. This method is based on the following considerations. In an earth-bound frame of reference, each body part theoretically follows a pure sine-like trajectory during one undulatory movement if two conditions are respected: (1) the swimming speed should be constant during the execution of one swimming movement and (2) the lateral amplitude of each body part should be small (Videler 1993). In reality, both conditions are violated. First, the thrust oscillates during one tail beat as the tail beats back and forth. Consequently, the swimming speed also fluctuates (Müller and van Leeuwen 2004). Variations in swimming speed are stronger in the viscous flow regime of small, slow swimmers than in the inertial flow regime of large, fast swimmers (Müller and van Leeuwen 2004). Second, the body wave amplitude increases from the pivot point to the tail (Videler 1981). The pivot point, located just behind the head, characterizes the position on the body where the smallest amplitude of lateral movements is usually observed. Consequently, the propulsive wave deviates moderately from a pure sine trajectory near this point and more markedly at the tail, where the amplitude is maximal. Based on the hypothesis that the motion of the various body parts deviates from a pure sine-like wave motion in the early developmental stages characterized by low *Re* values, we expect swimming movements to become increasingly sine-shaped during ontogeny, with increasing body length and swimming speed.

The aim of the present study was to describe qualitatively and quantitatively the development of swimming movements throughout the ontogeny of a supposed carangiform swimmer, the bronze corydoras (*Corydoras aeneus* (Gill, 1858)). We compared our results for *Corydoras aeneus* with those obtained for *Clarias gariepinus*, an anguilliform swimmer (Mauguit et al. 2010). We thus compared swimming ontogeny in two species belonging to the same order but having different swimming modes at adulthood.

Materials and methods

Larvae of *Corydoras aeneus* were bred in the laboratory. The temperature during ontogeny of the larvae was 25.0 ± 0.5 °C (mean ± SD) and the photoperiod was 12 h light : 12 h dark. Seventy-two hours posthatching (hPH), larvae were fed Nubil Fluids (JBL, Neuhofen, Germany) for 5 days. This food was gradually replaced with fresh nauplii of brine shrimp (*Artemia salina* (L., 1758)) (Novo Temia; JBL, Neuhofen, Germany). The larvae were fed 4–5 times a day during daylight hours exclusively. Fifteen larvae were randomly sampled at 0, 4, 8, 12, 16, 20, 24, 30, 36, 42, 48, 60, 72, 96, 120, 144, 168, 192, 216, 264, 312, 408, and 512 hPH. Five breeding *Corydoras aeneus* were also sampled to record the swimming movements of the last developmental stage.
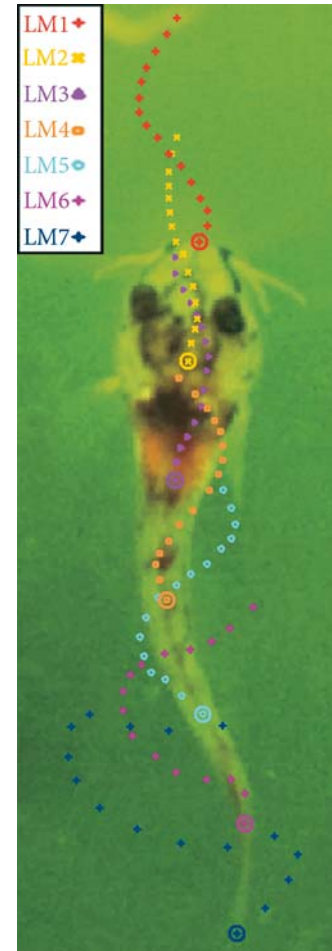
At each developmental stage, the movements of five batches of three larvae were recorded with a high-speed digital camera (RedLake MotionPro 2000; RedLake, San Diego, California, USA) at 500 frames/s (exposure time 200 μs). Thereafter, the larvae whose movements had been recorded were separated from the others. For the first developmental stages, the camera was mounted on a Stereozoom Microscope (Leica M10; Leica, Wetzlar, Germany) and the larvae were placed in a 75 mm × 25 mm aquarium. A 150 mm × 75 mm aquarium was used for fish exceeding 10 mm, and the camera was then used with a lens (Linos Mevis 25 mm, 1.6:16; Linos, Munich, Germany) and a 5 mm extension ring. Movements of adult fish were also recorded at 500 frames/s in a 500 mm × 250 mm tank. In this case, the 25 mm lens was used without an extension ring. In each case, the field was lit from the top and the bottom with two Volpi 6000-1 cold light sources (Volpi, Schlieren, Switzerland) and optical fibers. The depth of the water was at least five times the height of the fish body. At each developmental stage, swimming movements were recorded if the fish executed continuous swimming movements in a straight line and at constant speed. The fish were free to move in all directions and at variable swimming speeds. Only swimming movements executed after the first three tail strokes were recorded to avoid acceleration movements associated with the initiation of movement.

For larvae, a total of 68 sequences of one complete undulatory movement were analyzed in an earth-bound frame of reference with Midas version 2.1.1 (RedLake). Five were analyzed for adults. For each analyzed frame, the fish midline was determined by placing a succession of small linear segments between the snout and the tail tip. The fish midline was thus divided into six segments of equal length by placing seven landmarks equidistantly (LM1–LM7; Fig. 1). A preliminary study was carried out to determine the useful number of landmarks. Using more than seven points did not improve the precision of our results. Moreover, the use of seven landmarks allowed us to place the second one near the pivot point. The x axis was defined as the direction of fish displacement and the y axis was perpendicular to the x axis. The (x, y) coordinates of each landmark were mathematically transformed so that the x axis of the analysis referential coincided with the displacement axis of the fish. A second transformation was done to move the first point of the trajectory of each landmark to the x-axis origin ($x = 0$). The aim of these transformations was to use the same referential for analyzing the motions of each landmark independently of the landmark position or fish. For each sequence, direct and indirect parameters were determined and calculated.

The direct parameters used were total fish length (TL; mm), yolk-sac volume (Vv; mm^3), oscillatory movement period (T; s), relative swimming speed (U; TL/s), Reynolds number (Re), and the maximal amplitude of each landmark in each video sequence (A_{1-7}; %TL). The absolute swimming speed was calculated from the distance covered by the pivot point during the time it took to execute one tail beat. The results were thus divided by TL to obtain the relative swimming speed. Movements of the anterior part of the body contribute to increasing the drag of the fish, and hence, reduce its swimming efficiency (Lighthill 1975). Consequently, special attention was paid to the variation of head-movement amplitude throughout ontogeny in relation to swimming speed. The yolk-sac area (S) was determined with Vistametrix version 1.34 (SkillCrest LLC, Tucson, Arizona, USA). Yolk-sac volume was calculated as follows, assuming a spheroid shape: Vv = $(4/3) \times \pi \times (S \times \pi^{-1})^{1.5}$.

Three indirect parameters described in Mauguit et al. (2010) were used. A preliminary step must be carried out before one can determine the r^2_{mean} and CV of r^2 indices. From a distribution of the observed values of x, and knowing the movement amplitude (A_{1-7}) and its wavelength, sinusoids can be calculated for LM1–LM7 at each developmental stage. These sinusoids correspond to the theoretical ideal trajectories that each landmark should follow during execution of a complete undulatory movement, i.e., to the situation that should be observed at the adult stage (which is the last developmental stage). The paths observed for the various landmarks throughout ontogeny were compared with these theoretical sinusoids by determining the coefficient of determination (r^2) between the two curves. The coefficients of determination of LM1–LM7 (r^2_{1-7}) provided an objective index of the similarity between this motion and the adult sinusoid motion for each landmark placed on a fish. The r^2_{mean}, the mean of the r^2_1 to r^2_6 indices calculated for one fish, yielded a global index of the movement profile at a specific developmental stage. Swimming movements

Fig. 1. Picture of a swimming movement video sequence executed by a larva of bronze corydoras (*Corydoras aeneus*) measuring 10 mm total fish length. Each of the seven colored paths represents the trajectory of every landmark (LM1, LM2, …) during the execution of a complete undulatory swimming movement. Circles indicate the landmarks placed on the fish body.

were considered fully developed when $r^2_{mean} > 0.95$. The coefficient of variation of r^2 (CV of r^2), calculated with the r^2_1 to r^2_6 index values, was used to gauge whether at a given developmental stage the movement appeared to have reached the same level of organization in different parts of the body. The r^2_7 value was not used in the calculation of this index because LM7 was situated at the tip of the caudal fin and not on the body. The last index employed was the Strouhal number (St), which can be regarded as a propulsion efficiency index. It is calculated according to the formula: $St = f \times A_7 \times U^{-1}$, where f is the tail-beat frequency ($f = T^{-1}$; Hz), A_7 is the maximum amplitude of the tail movement (TL), and U is the relative swimming speed (TL/s). The St value describes how fast the tail is flapping relative to the fish forward speed. The swimming efficiency is optimal for adults (inertial flow regime) when the St value ranges from 0.2 to 0.4 (Taylor et al. 2003, Lauder and Tytell 2006).

The effects of growth and swimming speed (independent variables) on the variables (r^2_{mean}, CV of r^2, St, and amplitudes of LM1–LM7) were investigated by means of several multiple polynomial regressions of the third degree (the use

Fig. 2. Midline kinematics of larvae and adults of bronze corydoras (*Corydoras aeneus*) (right column) during cyclic swimming (fish-based frame of reference) and at different stages of ontogeny (A, B, C) or at adulthood (D). The superimposed midlines (time step maximum 6 ms) of one tail-beat cycle show the amplitude envelope of the body wave. Each amplitude envelope corresponds to the fish shown in the associated picture. In an amplitude envelope, the head is on the right. The amplitude is expressed as a proportion of total fish length (TL). *U*, relative swimming period.

of a larger degree of analysis does not give more information). The best-fit model was identified in a stepwise forward-selection manner and was selected based on lowest *p* value. Only significant model terms were included in the models (Student's *t* test, $p < 0.05$) and presented in the results. When both total length and swimming speed had significant effects on a parameter, the data were presented in surface plots with total fish length on the *x* axis and swimming speed on the *y* axis. On such plots, the values on the third axis, corresponding to the dependent variable, are given by a color code. The surface was fitted to the best of the points of observation by the weighted least squares method (McLain 1974).

Multiple polynomial regressions were also used to characterize the relationship between the total fish length, the yolk-sac absorption, and some of the other studied parameters (r^2_{mean}, CV of r^2, *St*, amplitudes of LM1–LM7).

Finally, we wanted to find out whether the biggest larvae had the same swimming characteristics as adults. As the ANOVA assumptions were not respected, nonparametric Mann–Whitney *U* tests were performed to compare the index values obtained for the five biggest larvae with the index value determined for the adults. The significance level was set at $p < 0.05$.

All the statistics were done with Statistica version 8.1 (Statsoft Inc., Tulsa, Oklahoma, USA). Values are mean ± SD, unless otherwise stated.

Results

Swimming mode of the adult stage

The size of studied adult fish was 59.6 ± 0.7 mm TL. Fish swam with tail-beat frequencies ranging from 3.1 to 8.6 Hz at speeds ranging from 3.07 to 4.87 TL/s.

The r^2_{mean} values were always >0.95, but they increased with increasing swimming speed ($F_{[1,3]} = 28.216$, $p = 0.013$, $R^2 = 0.9$). The mean CV of r^2 value was 3.34% ± 1.32%. The *St* values were mostly >0.7 (0.73 ± 0.14), which characterizes nonoptimal swimming movements. The *St* values were not significantly related to fish swimming speed ($F_{[1,3]} = 1.6489$, $p = 0.289$), although the lowest *St* value was associated with the fastest fish (0.55).

With increasing swimming speed, no change was observed in the maximal relative amplitude of the lateral displacement of the head ($F_{[1,3]} = 2.263$, $p = 0.230$) or tail ($F_{[1,3]} = 0.048$, $p = 0.841$). Figure 2D shows the envelope of amplitudes of an adult *Corydoras aeneus*. Based on this envelope (the amplitude of movement tends to increase exponentially in the posterior third party of the body) and as less than half of a propulsive wave was observed on the fish body, we conclude that the swimming mode of *Corydoras aeneus* is carangiform.
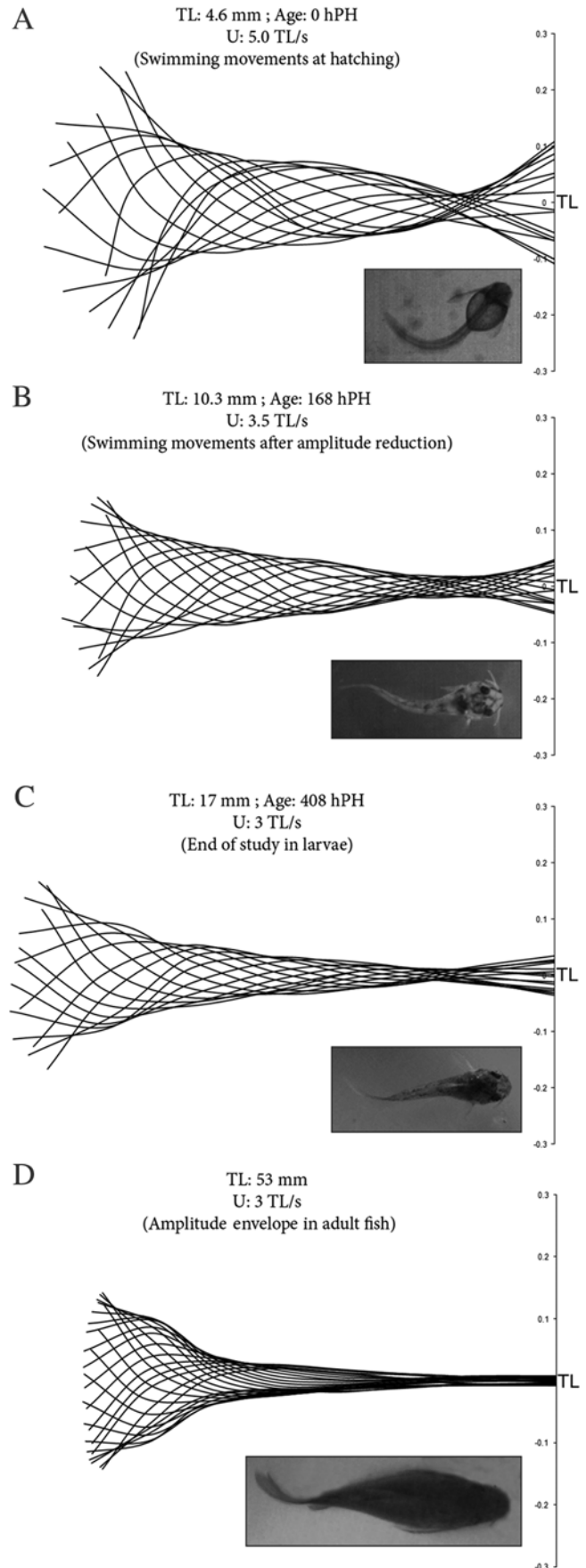
Table 1. Results of multiple polynomial regressions performed to characterize the effects of size (total fish length, TL) and relative swimming speed (U) on the evolution of the mean coefficient of determination (r^2_{mean}), coefficient of variation of r^2 (CVof r^2), and Strouhal number (St) indices in bronze corydoras (*Corydoras aeneus*).

Determinant	Partial regression coefficient	Standard error on estimate	0.95 confidence interval	Significance of the variables (Student's t test)		
				t	df	p
r^2_{mean} ($F_{[4,63]}$ = 12.824, p < 0.001)						
Intercept	–0.266	0.042	–0.183 to –0.349	–6.30	63	<0.001
TL (mm)	0.064	0.013	0.090 to 0.038	4.84	63	<0.001
TL^2 (mm^2)	–0.006	0.001	–0.003 to –0.008	–4.32	63	<0.001
U (TL/s)	0.02	0.001	0.003 to 0.001	4.34	63	<0.001
TL^3 (mm^3)	0.000146	0.000	0.000220 to 0.0000731	3.92	63	<0.001
CV of r^2 ($F_{[4,63]}$ = 10.481, p < 0.001)						
Intercept	0.301	0.060	0.418 to 0.183	5.01	63	<0.001
TL (mm)	–0.069	0.019	–0.032 to –0.106	–3.67	63	<0.001
TL^2 (mm^2)	0.006	0.002	0.009 to 0.002	3.17	63	<0.001
U (TL/s)	–0.003	0.001	–0.001 to –0.004	–3.75	63	<0.001
TL^3 (mm^3)	–0.000149	0.0000531	–0.0000448 to –0.000253	–2.80	63	<0.001
St ($F_{[5,62]}$ = 29.430, p < 0.001)						
Intercept	3.909965	0.516044	4.921 to 2.899	7.58	62	<0.001
TL (mm)	–0.545991	0.150240	–0.252 to –0.840	–3.63	62	<0.001
U (TL/s)	–0.154651	0.027262	–0.101 to –0.208	–5.67	62	<0.001
TL^2 (mm^2)	0.041738	0.014423	0.070 to 0.013	2.89	62	0.0052
U^2 (TL^2/s^2)	0.006000	0.001490	0.009 to 0.003	4.03	62	<0.001
TL^3 (mm^3)	–0.001044	0.000422	–0.000216 to –0.00187	–2.47	62	0.0162

Note: Total variances explained for r^2_{mean}, CV of r^2, and St were 45%, 40%, and 70%, respectively.

Ontogeny of swimming movements

At hatching, larvae measured 4.38 ± 0.39 mm TL and possessed a mean yolk-sac volume of 1.02 ± 0.16 mm^3. The yolk sac was completely absorbed between 72 and 96 hPH (5% of the yolk-sac volume was still left at 72 hPH). The larval size was 7.24 ± 0.21 mm at 96 hPH when absorption was complete. Growth was linear (y = 0.0301x + 4.5729; r = 0.99, p < 0.001) and the fish reached a size of 18.73 ± 0.18 mm TL at 512 hPH.

During the experiment, tail-beat frequencies ranged from 5 to 45 Hz. No linear relationship existed between size and tail-beat frequency ($F_{[1,66]}$ = 3.32, p = 0.073), but the highest tail-beat frequencies were observed in larvae having reached 6–8 mm TL in size (U = 355.5, p = 0.025). The relative swimming speed ranged from 1.26 to 17.02 TL/s. This range was observed throughout ontogeny; no significant relationship was found between size and swimming speed ($F_{[1,66]}$ = 0.13, p = 0.72).

Swimming movements were established soon after hatching, i.e., between 0 and 4 hPH. The landmarks followed sinusoidal paths during execution of these movements (r^2_{mean} > 0.95). The r^2_{mean} coefficient, however, increased during larval growth (Table 1) until it reached a plateau at approximately 8 mm TL (r^2_{mean} = 0.98; Fig. 3A). At hatching, some landmarks (LM2–LM5) showed more sinusoidal trajectories than others (CV of r^2 = 9.37% ± 2.2%), but all landmarks acquired good sinusoidal trajectories by the time the larvae reached a size of 8 mm TL (CV of r^2 = 1.83% ± 0.93%; Fig. 3B). The St values were high at hatching (St = 1.52 ± 0.26) and decreased during growth (Table 1). This decrease was pronounced until the larvae reached a size of 8 mm TL (St =

1.01 ± 0.18; Fig. 3C). Thereafter, the St value decreased more slowly, stabilizing at 0.69 ± 0.16 in larvae measuring 18.73 ± 0.18 mm TL.

Directly after hatching, the fish larvae used anguilliform swimming movements: all landmarks except LM2 executed large lateral displacements during one tail beat (Fig. 2A). As the larvae grew to about 8 mm TL, the maximal movement amplitudes of all landmarks decreased (Figs. 2B, 4). The smallest amplitude was always observed for LM2, located near the pivot point. The amplitudes of all landmarks continued to decrease in fish longer than 8 mm TL, but the decrease was less rapid than what was observed in larvae less than 8 mm TL, especially for LM3–LM6 (Fig. 2C). In comparison with the amplitude envelope of adult fish (Fig. 2D), it seems that the transition from an anguilliform to a carangiform swimming mode began just before the fish reached 17 mm TL.

The swimming speed affected all the indirect parameters significantly (i.e., r^2_{mean}, CV of r^2, St; Table 1). During ontogeny, a positive correlation was observed between r^2_{mean} and swimming speed (Fig. 3A, Table 1). An increase in swimming speed induced homogenization of the path followed by the landmarks, i.e., a decrease in CV of r^2 (Fig. 3B, Table 1). Variations in St values also depended on swimming speed (Table 1), which decreased with increasing swimming speed (Fig. 3C).

The swimming speed affected the maximal amplitude of the various landmarks differently. An increase in swimming speed had no effect on the amplitudes of LM1, LM2, and LM7 (i.e., the landmarks on the head, pivot point, and tail, respectively) (Table 2). In contrast, the maximal relative

Fig. 3. Contour plot representing the changes in (A) mean coefficient of determination (r^2_{mean}), (B) coefficient of variation of r^2 (CV of r^2), and (C) Strouhal number (St) as a function of total fish length (TL) and relative swimming speed of larvae of bronze corydoras (*Corydoras aeneus*). The index value increases from dark green to dark red. The white circles represent observations made during the present study; each circle corresponds to one fish. These data were used to fit the isoclines by using the weighted least squares distance method. In A, the blue line represents the threshold value of 0.95. White circles located to the left of this line correspond to fish that did not execute fully developed swimming movements, whereas those to the right of this line correspond to fish with established swimming movements.
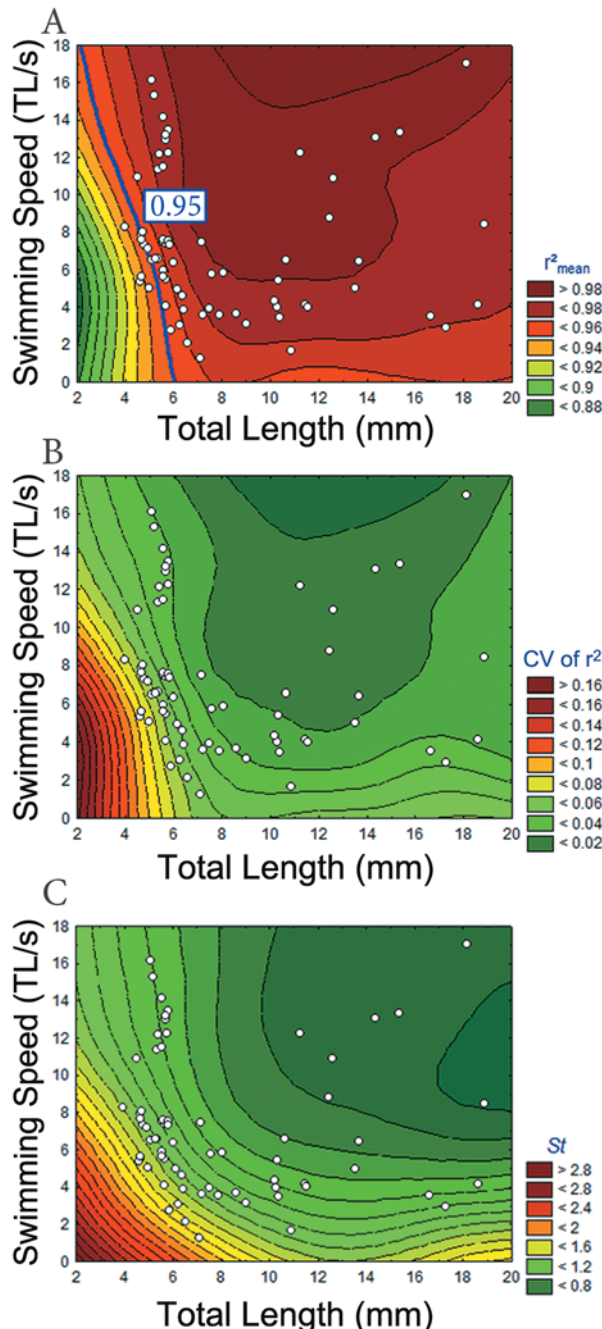
lateral-movement amplitudes observed for LM3–LM6 increased with increasing swimming speed, but only in larvae measuring more than 8 mm TL (Fig. 4).

Yolk-sac absorption affected the motion of the landmarks by improving the trajectories of the landmarks. Multiple polynomial regressions showed an influence of both growth and yolk-sac absorption on the indirect parameters r^2_{mean}, CV of r^2, and St. Unlike yolk-sac absorption, growth did not affect the indices (Table 3). Furthermore, yolk-sac absorption had no effect on the St index (Table 3).

Landmark amplitudes were also affected by yolk-sac absorption. A strong negative correlation was found between yolk-sac absorption and reduction of the amplitudes of LM1–LM6 (Table 3). Our statistical analysis confirmed, however, that size is also an important factor, with effects on movement amplitudes throughout ontogeny (Table 2).

The theoretical change in hydrodynamic flow regime, from intermediate to inertial ($Re > 1000$), occurs at approximately 12 mm TL. The r^2_{mean} increased (from around 0.91 to 0.98) and the CV of r^2 decreased (from around 0.12 to 0.02) with increasing Re values, both reaching a plateau before the flow regime transition at $Re = 1000$ (Figs. 5A, 5B). St value decreased strongly, from 2.1 to around 0.8, before the theoretical limit between intermediate and inertial flow regimes (Fig. 5C). Thereafter, the St value continued to decrease slowly and stabilized at around 0.7.

Comparisons between adults and the five biggest larvae

No difference was observed between the five biggest larvae and the adults in terms of r^2_{mean} (Mann–Whitney U test, $U_{[9]} = -1.567$, $p = 0.117$), CV of r^2 ($U_{[9]} = 0.94$, $p = 0.347$), and St ($U_{[9]} = -0.522$, $p = 0.60$) indices. Differences in maximal movement amplitude were observed for LM1 (Mann–Whitney U test, $U_{[9]} = -2.193$, $p = 0.028$), LM3 ($U_{[9]} = -2.611$, $p = 0.009$), LM4 ($U_{[9]} = -2.402$, $p = 0.016$), and LM7 ($U_{[9]} = 1.984$, $p = 0.047$). The relative amplitudes of these landmarks were smaller in the adults than in the biggest larvae (Figs. 2C–2D), confirming that the swimming mode transition had just begun in the biggest larvae (18.73 ± 0.18 mm TL) and had yet to continue. The swimming mode transition was observed well after the flow regime change.

Discussion

As expected, swimming activity and performance changed during ontogeny. During the first hours posthatching, larvae of *Corydoras aeneus* can reach very high tail-beat frequencies (45 Hz). Müller and van Leeuwen (2004), who observed a tail-beat frequency of 100 Hz in *D. rerio*, hypothesize that young larvae possess high-performance adaptations such as thin myofibrils, a considerable amount of sarcoplasmic reticulum, and a high myosin ATPase rate. Moreover, Focant et al. (1999) observed a rapid change in muscle protein isoforms in three catfish species (*Clarias gariepinus*, Golden Nile catfish (*Chrysichthys auratus* (Geoffroy Saint-Hilaire, 1809)), and Sampa (*Heterobranchus longifilis* Valenciennes in Cuvier and Valenciennes, 1840)) during the first weeks of larval development. Such observations, in two distant species like *Corydoras aeneus* and *D. rerio*, highlight the importance

Fig. 4. Contour plot showing the movement amplitudes of landmarks 2 to 7 (LM2–LM7) on larvae of bronze corydoras (*Corydoras aeneus*) as a function of total fish length (TL) and relative swimming speed. The amplitude increases when the colored area changes from dark green to dark red. The colored scale is expressed as a proportion of TL. The white circles represent observations made during the present study; each circle corresponds to one fish.
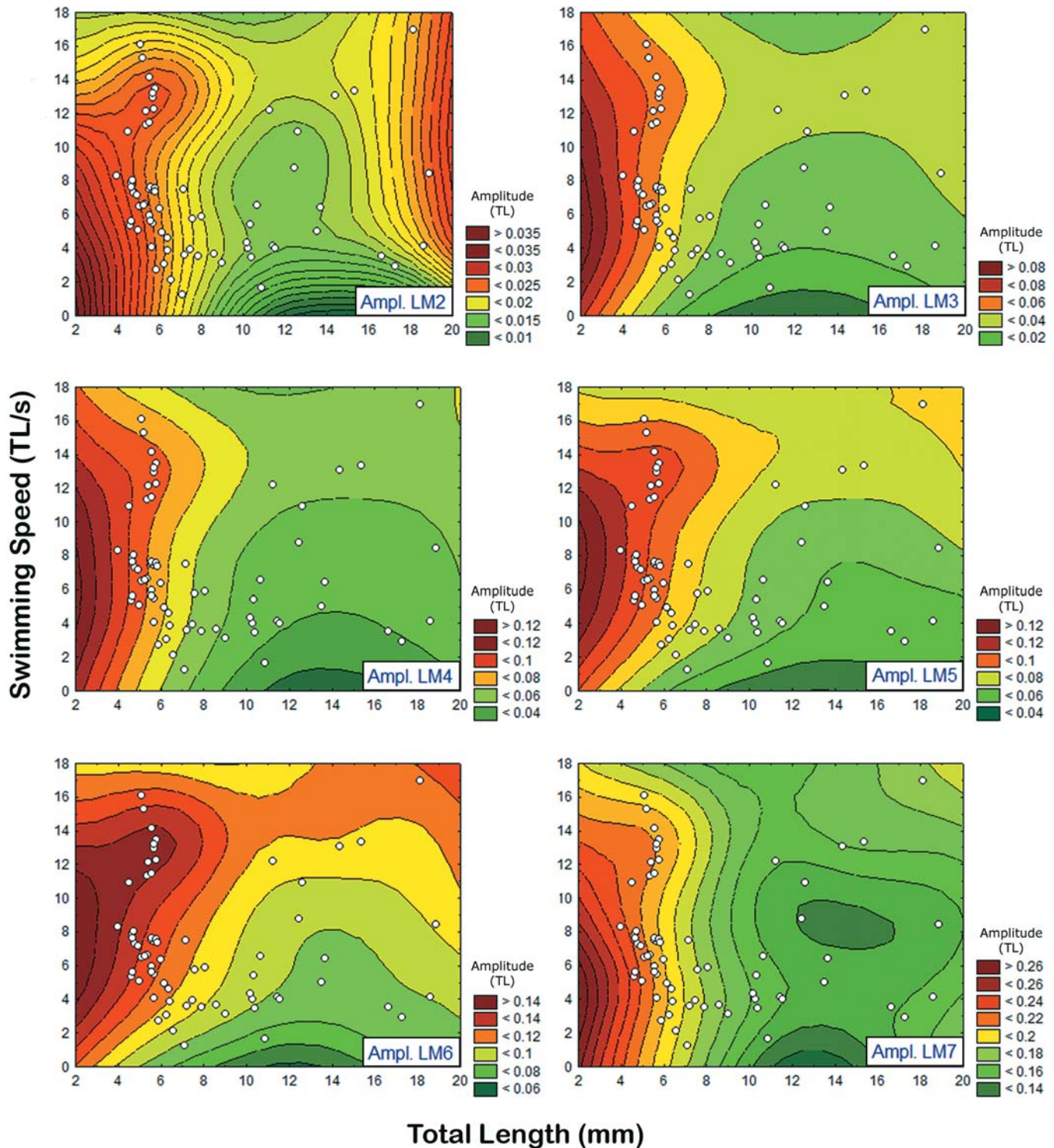
of muscle physiology in fish swimming ontogeny during the first developmental stage.

The ontogeny of swimming movements in catfish, and more precisely in *Clarias gariepinus*, was studied in an earlier paper (Mauguit et al. 2010). This earlier paper enables

us to compare *Corydoras aeneus*, a carangiform swimmer, with *Clarias gariepinus*, an anguilliform swimmer.

Adult American eels (*Anguilla rostrata* (Lesueur, 1817)) use the anguilliform swimming mode, which is adapted to all types of hydrodynamic flow regime (Gray and Hancock

Table 2. Results of multiple polynomial regressions performed to characterize the effects of size (total fish length, TL) and relative swimming speed (U) on the evolution of the amplitude of each landmark (LM) in bronze corydoras (*Corydoras aeneus*).

Determinant	Partial regression coefficient	Standard error on estimate	0.95 confidence interval	Significance of the variables (Student's t test)		
				t	df	p
Amplitude LM1 ($F_{[3,63[} = 63.546, p < 0.001$)						
Intercept	0.271	0.028	0.217 to 0.325	9.83	63	<0.001
TL (mm)	−0.056	0.009	−0.074 to −0.039	−6.27	63	<0.001
TL^2 (mm^2)	0.004	0.001	0.003 to 0.006	5.00	63	<0.001
TL^3 (mm^3)	−0.000107	0.0000259	−0.000158 to −0.0000565	−4.14	63	<0.001
Amplitude LM2 ($F_{[2,65]} = 15.08, p < 0.001$)						
Intercept	0.036	0.003	0.031 to 0.042	13.0	65	<0.001
TL (mm)	−0.002		−0.003 to −0.001	−4.94	65	<0.001
TL^2 (mm^2)	0.00000457	0.00000118	0.00000227 to 0.00000688	3.89	65	<0.001
Amplitude LM3 ($F_{[4,63]} = 58.810, p < 0.001$)						
Intercept	0.157	0.021	0.117 to 0.198	7.58	63	<0.001
TL (mm)	−0.032	0.006	−0.045 to −0.019	−4.93	63	<0.001
TL^2 (mm^2)	0.002	0.001	0.001 to 0.004	3.82	63	<0.001
U (TL/s)	0.001	0.000269	0.000381 to 0.001	3.37	63	0.001
TL^3 (mm^3)	−0.0000574	0.0000183	−0.0000934 to −0.0000215	−3.13	63	0.003
Amplitude LM4 ($F_{[4,63]} = 63.655, p < 0.001$)						
Intercept	0.130	0.009	0.112 to 0.148	14.22	63	<0.001
TL (mm)	−0.013	0.002	−0.017 to −0.010	−7.46	63	<0.001
TL^2 (mm^2)	0.000470	0.0000834	0.000306 to 0.000633	5.63	63	<0.001
U (TL/s)	0.001	0.000333	0.000460 to 0.00176	3.34	63	0.001
Amplitude LM5 ($F_{[2,65]} = 40.820, p < 0.001$)						
Intercept	0.098	0.005	0.088 to 0.108	19.0	65	<0.001
TL (mm)	−0.003	0.000434	−0.004 to −0.003	−7.72	65	<0.001
U (TL/s)	0.002	0.000450	0.001 to 0.003	4.34	65	<0.001
Amplitude LM6 ($F_{[3,64]} = 29.212, p < 0.001$)						
Intercept	0.163	0.015	0.134 to 0.193	10.97	64	<0.001
TL (mm)	−0.012	0.003	−0.018 to −0.007	−4.20	64	<0.001
U (TL/s)	0.002	0.001	0.001 to 0.003	4.45	64	<0.001
TL^2 (mm^2)	0.000427	0.000136	0.000160 to 0.000695	3.14	64	0.003
Amplitude LM7 ($F_{[2,65]} = 58.673, p < 0.001$)						
Intercept	0.304	0.015	0.275 to 0.334	20.28	65	<0.001
TL (mm)	−0.022	0.003	−0.028 to −0.015	−6.60	65	<0.001
TL^2 (mm^2)	0.001	0.000154	0.000461 to 0.00106	4.96	65	<0.001

Note: Total variances explained for amplitudes of LM1–LM7 were 64%, 30%, 79%, 75%, 56%, 58%, and 64%, respectively.

1955; Lighthill 1969; Webb and Weihs 1986) and specifically to the viscous and intermediate regimes. In this last case, thrust is generated according to both the resistive and the reactive models (Webb and Weihs 1986). Larvae of *Corydoras aeneus* (present study) and *Clarias gariepinus* (Mauguit et al. 2010) have an anguilliform swimming mode when confronted with the intermediary flow regime ($10 < Re < 10\,000$). Their bodies are well adapted to such hydrodynamic conditions, thanks to their great flexibility and their deep vertical dimensions given by the presence of the finfold. These two properties allow the larvae to increase the mass of accelerated water. The similarity of body shape between these larvae and adult *A. rostrata* is obvious. Moreover, hydrodynamic similarities are also observed: Müller et al. (2008) reported that adult *A. rostrata* and larval *D. rerio* leave a similar wake when swimming.

The first major difference between the two species is ob-served immediately at hatching: larvae of *Corydoras aeneus* can swim, whereas larvae of *Clarias garipinus* cannot swim. The incubation time is approximately 24 h for *Clarias gariepinus* (Mauguit et al. 2010) and 72 h for *Corydoras aeneus*. Despite this difference, both species hatch at the same stage of morphological development: the mouth, the anus, and the opercular cavity are closed (Legendre and Teugels 1991; Osman et al. 2008; Huysentruyt et al. 2009). Both species possess a finfold, but only larvae of *Corydoras aeneus* possess pectoral fins. These fins are not supported by fin rays and can be viewed as large skin folds (Huysentruyt et al. 2009). The presence of these fins is very important, as they may help to reduce the lateral movement of the head during execution of swimming movements (Batty 1981; Thorsen et al. 2004). Their presence may explain the relative quality of the swimming movements observed at hatching for *Corydoras aeneus* ($r^2_{mean} > 0.95$). *Clarias gariepinus* reaches

Table 3. Results of multiple polynomial regressions performed to characterize the effects of size (total fish length, TL) and yolk-sac absorption (Vv) on the evolution of the mean coefficient of determination (r^2_{mean}), coefficient of variation of r^2 (CV of r^2), Strouhal number (St) indices, and maximal amplitudes of landmarks 1–7 (LM1–LM7) in bronze corydoras (*Corydoras aeneus*).

| Determinant	Partial regression coefficient	Standard error on estimate	0.95 confidence interval	Significance of the variables (Student's t test)		
				t	df	p
r^2_{mean} ($F_{[1,66]}$ = 33.575, p < 0.001)						
Intercept	–0.024406	0.002512	–0.019 to –0.029	–9.71	66	<0.001
Vv (mm³)	–0.035581	0.006141	–0.024 to –0.048	–5.79	66	<0.001
CV of r^2 ($F_{[1,66]}$ = 26.418, p < 0.001)						
Intercept	0.026269	0.003915	0.034 to 0.019	6.71	66	<0.001
Vv (mm³)	0.041328	0.008041	0.057 to 0.026	5.14	66	<0.001
St ($F_{[1,66]}$ = 26.418, p < 0.001)						
Intercept	0.733855	0.035394	0.803 to 0.664	20.7	66	<0.001
TL (mm)	–0.021269	0.003947	–0.014 to –0.029	–5.39	66	<0.001
Amplitude LM1 ($F_{[2,65]}$ = 105.98, p < 0.001)						
Intercept	0.045089	0.001903	0.049 to 0.041	23.7	65	<0.001
Vv (mm³)	0.075542	0.011920	0.099 to 0.052	6.34	65	<0.001
Vv² (mm⁶)	–0.025868	0.012859	–0.001 to –0.051	–2.01	65	0.048
Amplitude LM2 ($F_{[6,61]}$ = 8.4151, p < 0.001)						
Vv (mm³)	0.061141	0.017995	0.096 to 0.026	3.40	61	0.001
Vv² (mm⁶)	–0.114420	0.037561	–0.041 to –0.188	–3.05	61	0.003
Vv³ (mm⁹)	0.060052	0.023022	0.105 to 0.015	2.61	61	0.011
Amplitude LM3 ($F_{[3,64]}$ = 85.105, p < 0.001)						
Intercept	0.026740	0.001343	0.029 to 0.024	19.9	64	<0.001
Vv (mm³)	0.132375	0.020840	0.173 to 0.092	6.35	64	<0.001
Vv² (mm⁶)	–0.211210	0.053481	–0.106 to –0.316	–3.95	64	<0.001
Vv³ (mm⁹)	0.114151	0.033929	0.181 to 0.048	3.36	64	0.001
Amplitude LM4 ($F_{[5,62]}$ = 41.048, p < 0.001)						
Intercept	0.079727	0.017893	0.115 to 0.045	4.46	62	<0.001
Vv (mm³)	0.109554	0.035823	0.180 to 0.039	3.06	62	0.003
Vv² (mm⁶)	–0.170540	0.078284	–0.017 to –0.324	–2.18	62	0.033
Amplitude LM5 ($F_{[4,63]}$ = 26.802, p < 0.001)						
Intercept	0.074957	0.007442	0.090 to 0.060	10.1	63	<0.001
Vv (mm³)	0.151022	0.041486	0.232 to 0.070	3.64	63	<0.001
Vv² (mm⁶)	–0.240909	0.098697	–0.047 to –0.434	–2.44	63	0.017
Amplitude LM6 ($F_{[3,64]}$ = 23.475, p < 0.001)						
Intercept	0.096402	0.003083	0.102 to 0.090	31.3	64	<0.001
Vv (mm³)	0.176905	0.047847	0.271 to 0.083	3.70	64	<0.001
Vv² (mm⁶)	–0.273792	0.122789	–0.033 to –0.514	–2.23	64	0.029
Amplitude LM7 ($F_{[4,63]}$ = 30.970, p < 0.001)						
Intercept	0.238506	0.023738	0.285 to 0.192	10.0	63	<0.001
TL (mm)	–0.009044	0.003126	–0.003 to –0.015	–2.90	63	0.005
TL³ (mm³)	0.000014	0.000006	0.0000261 to 0.00000128	2.16	63	0.034

Note: Total variances explained for r^2_{mean}, CV of r^2, St, and amplitudes of LM1–LM7 were 34%, 29%, 31%, 77%, 45%, 80%, 77%, 63%, 42%, and 66%, respectively.

the same level of swimming movements only 42–48 hPH (Mauguit et al. 2010). At this stage, *Clarias gariepinus* does not possess any pectoral fins, as the first outlines of these structures do not appear until about 96 hPH (Q. Mauguit, personal observation). Consequently, pectoral fins are not involved in the establishment of swimming movements in *Clarias gariepinus*.

The relationship between St value and swimming efficiency is well known in adult fish, but little information is available for larvae. Because information is lacking regarding the interpretation of the St value in a noninertial flow regime, we cannot interpret our results obtained for the larvae in terms of efficiency. However, we can compare the variation of this index throughout the ontogeny of the two catfishes. The maximal St value observed for the first swimming movements was 1.8 for *Corydoras aeneus* (present study) and 2.52 for *Clarias gariepinus* (Mauguit et al. 2010). However, the St values decreased rapidly (to about

Fig. 5. Plots of (A) mean coefficient of determination (r^2_{mean}), (B) coefficient of variation of r^2 (CV of r^2), and (C) Strouhal number (St) as a function of Reynolds number (Re) in larvae of bronze corydoras (*Corydoras aeneus*). The vertical lines indicate the theoretical shift in flow regime. Each circle corresponds to a measurement carried out on one fish.
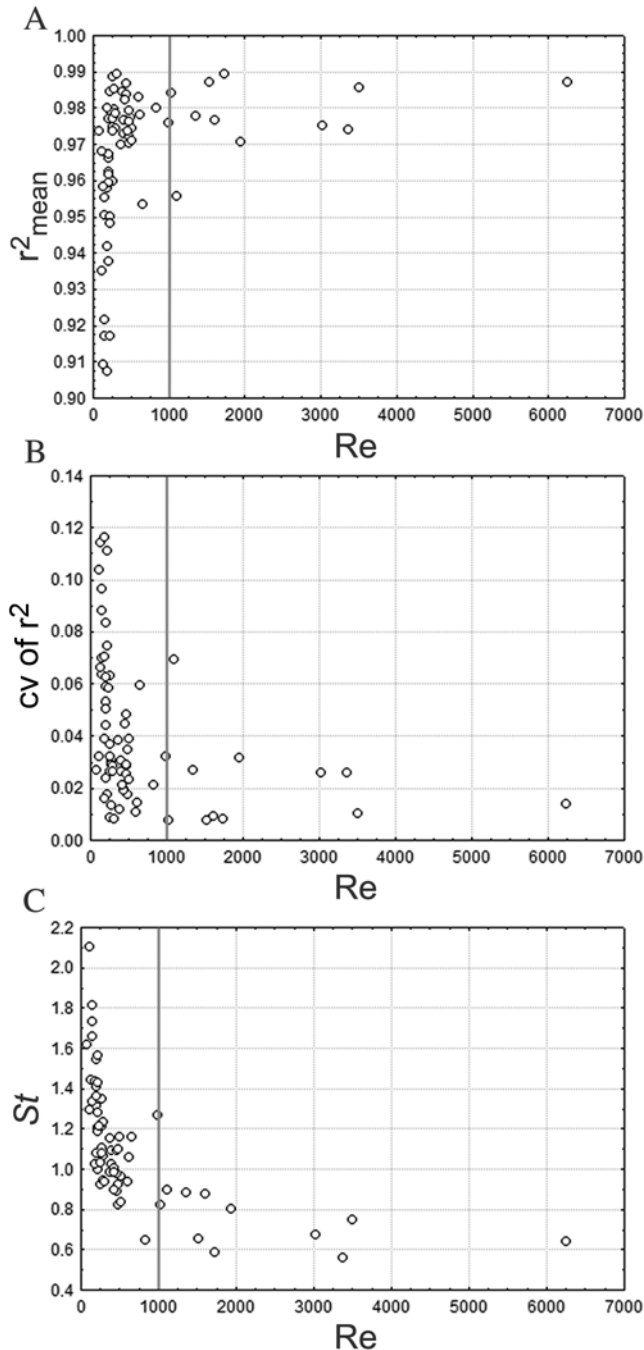
50% of the initial value) until larvae of *Corydoras aeneus* reached about 8 mm TL (this study) or until larvae of *Clarias gariepinus* reached about 12 mm TL (Mauguit et al. 2010). This decrease in St value may be linked to the decrease in the maximal amplitude of LM7 in both larvae of both species (Mauguit et al. 2010; present study). The reduc-

tion in both head and body amplitude during swimming allows better penetration of the water (Batty 1981), and consequently, an increase in efficiency of swimming movement. The larvae of both species show decreasing St values with increasing swimming speed, which might be related to the way the Re value varies. At high speed, the Re value increases considerably in swimming larvae, which means that the influence of viscous forces decreases. Consequently, total drag decreases.

A total length of 8 and 12 mm seems to be a crucial step in the ontogeny of swimming in *Corydoras aeneus* and *Clarias gariepinus*, respectively. At this stage, the ossification only starts in the anterior part of the vertebral column in *Clarias gariepinus* (Q. Mauguit, personal observation), whereas almost all of the vertebrae are fully ossified in *Corydoras aeneus* (Huysentruyt et al. 2009; Q. Mauguit, personal observation). The caudal skeleton is at the same level of development in both species; hypurals are fully developed in their cartilaginous form and their anterior halves are ossified and ossified fin rays were observed (Huysentruyt et al. 2009; Q. Mauguit, personal observation). The dorsal fin was not differentiated from the finfold in both species (Huysentruyt et al. 2009; Q. Mauguit, personal observation). Consequently, the complete ossification of the postcranial skeleton does not seem to be a requirement in the acquisition of fully efficient swimming movements. The results of van Raamsdonk et al. (1982, 1983) may provide an additional explanation of what happens when *Corydoras aeneus* reaches 8 mm TL. In their studies on the differentiation of muscle fiber types in *D. rerio*, van Raamsdonk et al. (1982, 1983) reported that adult-type red muscle fibers begin to develop, and that the number of white and intermediate muscle fibers increases very rapidly in specimens measuring 8–10 mm TL. A similar muscle development profile in *Corydoras aeneus* and *Clarias gariepinus* might be related to our kinematic data. This underlines the crucial role of muscle development during swimming ontogeny.

Various events are related to variations in swimming speed. In *Corydoras aeneus* longer than 8 mm TL (including adults), the maximal amplitudes of landmarks placed between the pivot point and the tail (LM4–LM6) increase when the swimming speed increases. In *Clarias gariepinus* longer than 12 mm TL, the amplitudes of LM3–LM6 also increase until the fish reaches a swimming speed of 4.5 TL/s. Thereafter, the amplitudes tend to decrease with increasing swimming speed (Mauguit et al. 2010). By increasing body rigidity, adult fish can control their swimming speed by maintaining the wavelength of the wave of curvature at a constant value (Mchenry et al. 1995). The maximal amplitude of the head (LM1) and tail (LM7) does not change with swimming speed in *Corydoras aeneus* as it does in Atlantic cod (*Gadus morhua* L.,1758)) (Videler and Wardle 1991) and *A. rostrata* (Tytell 2004). This contrasts partly with the situation observed in *Clarias gariepinus*, where the amplitude of the head depends on the swimming speed (Mauguit et al. 2010).

The presence of the yolk sac at hatching does not prevent the execution of sinusoidal movements in *Corydoras aeneus*. Yet during the phase of absorption of the vitelline reserve, the trajectories followed by the landmarks tended to become a little bit more sinusoidal, as r^2_{mean} index increased. This

phenomenon was observed all over the body, as the values of the CV of r^2 index decreased during the same period. In *Clarias gariepinus*, sinusoidal movements do not appear until the yolk sac is almost totally absorbed (i.e., 95% total absorption; Mauguit et al. 2010). The yolk sac can throw the fish off balance. In *Corydoras aeneus*, the presence of the pectoral fins may play an important role in stabilization during swimming. Moreover, the results of the multiple polynomial regressions indicated that the absorption of the yolk sac did not significantly influence the efficiency of the locomotor movements of this species. Indeed, swimming efficiency was only correlated to fish growth.

No major event was observed at the theoretical flow regime transition ($Re > 1000$). In the intermediate flow regime, the values of all three indirect indices strongly changed as the value of Re increased. Yet the variations of these indices were relatively minor before the flow regime transition. Our study confirms that this transition has no effect on the ontogeny of swimming movements, as also highlighted in *Clarias gariepinus* (Mauguit et al. 2010) and *D. rerio* (Lauder and Tytell 2006).

The St values of adult *Corydoras aeneus* and of the longest larvae did not fall within the range of 0.2–0.4, which corresponds to the theoretical maximal efficiency (Read et al. 2003; Taylor et al. 2003). Information regarding St values is available only for *A. rostrata* and for pelagic fish (e.g., mackerel (Scombridae), mullet (Mugilidae), cod (Gadidae), jack (Carangidae), carp (Cyprinidae), and trout and salmon (Salmonidae); Taylor et al. 2003). All these species swim with St values within the optimal range. Yet some species, such as the Chinook salmon (*Oncorhynchus tshawytscha* (Walbaum in Artedi, 1792)) can swim at low speed (0.5 LT/s) without being in the optimal range (Lauder and Tytell 2006). Two hypotheses have been proposed by Lauder and Tytell (2006): swimming movements might be inefficient at low swimming speed or the St value might not capture the complexities of swimming efficiency at low speed. Here, however, the adult *Corydoras aeneus* specimens whose movements were recorded did not swim slowly (<1 TL/s), so another explanation is required. The St value does not vary with swimming speed in adult *Corydoras aeneus*; however, because the lowest St value was observed in the fastest *Corydoras aeneus* and because the swimming efficiency of *Clarias gariepinus* is known to correlate positively with swimming speed (Mauguit et al. 2010), we hypothesize that fish from these species swimming at a greater than usual speed will be characterized by an optimal St value. Both of these catfishes are benthopelagic (Burgess 1989), as such their swimming movements are used mainly for foraging and not for covering long distances at a sustained speed. Consequently, they probably do not need to be fully efficient according to a theoretical definition. The St value may thus become optimal when the fish need to rapidly execute behaviors that are essential to their survival, such as avoiding predators or catching food. A more complete study should be carried out on adult *Corydoras aeneus* because the fish in our study were free to choose their own swimming speed, which was probably their routine swimming speed. We do not have any information on what the St value would be at low (<1 TL/s) or high (>5 TL/s) swimming speed.

References

Batty, R.S. 1981. Locomotion of plaice larvae. Symp. Zool. Soc. Lond. **48**: 53–69.

Batty, R.S. 1983. Observation of fish larvae in the dark with television and infra-red illumination. Mar. Biol. (Berl.), **76**(1): 105–107. doi:10.1007/BF00393061.

Batty, R.S. 1984. Development of swimming movements and musculature of larval herring (*Clupea harengus*). J. Exp. Biol. **110**: 217–229. PMID:6747536.

Burgess, W.E. 1989. An atlas of freshwater and marine catfishes: a preliminary survey of the Siluriformes. T.F.H. Publications, Inc., Neptune City, N.J.

Carrier, D.R. 1996. Ontogenetic limits on locomotor performance. Physiol. Zool. **69**: 467–488.

Focant, B., Mélot, F., Collin, S., Chikou, A., Vandewalle, P., and Huriaux, F. 1999. Muscle parvalbumin isoforms of *Clarias gariepinus*, *Heterobranchus longifilis* and *Chrysichthys auratus*: isolation, characterization and expression during development. J. Fish Biol. **54**: 832–851. doi:10.1111/j.1095-8649.1999.tb02036.x.

Fontaine, E., Lentink, D., Kranenbarg, S., Müller, U.K., van Leeuwen, J.L., Barr, A.H., and Burdick, J.W. 2008. Automated visual tracking for studying the ontogeny of zebrafish swimming. J. Exp. Biol. **211**(8): 1305–1316. doi:10.1242/jeb.010272. PMID:18375855.

Fuiman, L.A., and Batty, R.S. 1997. What a drag it is getting cold: partitioning the physical and physiological effects of temperature on fish swimming. J. Exp. Biol. **200**(12): 1745–1755. PMID:9319652.

Fuiman, L.A., and Webb, P.W. 1988. Ontogeny of routine swimming activity and performance in *Zebra danio* (Teleostei; Cyprinidae). Anim. Behav. **36**(1): 250–261. doi:10.1016/S0003-3472(88)80268-9.

Gray, J. 1933. Studies in animal locomotion: I. The movement of fish with special reference to the eel. J. Exp. Biol. **10**: 88–104.

Gray, J., and Hancock, G.J. 1955. The propulsion of sea-urchin spermatozoa. J. Exp. Biol. **32**: 775–801.

Hale, M.E. 1999. Locomotor mechanics during early life history: effects of size and ontogeny on fast-start performance of salmonid fishes. J. Exp. Biol. **202**(11): 1465–1479. PMID:10229693.

Huysentruyt, F., Moerkerke, B., Devaere, S., and Adriaens, D. 2009. Early development and allometric growth in the armoured catfish *Corydoras aeneus* (Gill, 1858). Hydrobiologia, **627**(1): 45–54. doi:10.1007/s10750-009-9714-z.

Lauder, G.V., and Tytell, E.D. 2006. Hydrodynamics of undulatory propulsion. *In* Fish biomechanics. *Edited by* R.E. Shadwick and G.V. Lauder. Elsevier, New York. pp. 425–468.

Legendre, M., and Teugels, G.G. 1991. Développement et tolérance à la température des oeufs de *Heterobranchus longifilis*, et comparaison des développements larvaires de *H. longifilis* et de *Clarias gariepinus* (Teleostei, Clariidae). Aquat. Living Resour. **4**(4): 227–240. doi:10.1051/alr:1991024.

Lighthill, M.J. 1969. Hydrodynamics of aquatic animal propulsion.

Annu. Rev. Fluid Mech. **1**(1): 413–446. doi:10.1146/annurev.fl.
01.010169.002213.

Lighthill, J. 1975. Mathematical biofluiddynamics. SIAM, Philadel-
phia, Pa.

Long, J.H., and Nipper, K.S. 1996. The importance of body stiff-
ness in undulatory propulsion. Am. Zool. **36**: 678–694.

Long, J.H., Mchenry, M.J., and Boetticher, N.C. 1994. Undulatory
swimming: how traveling waves are produced and modulated in
sunfish (*Lepomis gibbosus*). J. Exp. Biol. **192**(1): 129–145.
PMID:9317485.

Mauguit, Q., Gennotte, V., Becco, C., Baras, E., Vandewalle, N.,
and Vandewalle, P. 2010. Ontogeny of swimming movements
in the catfish *Clarias gariepinus*. Open Fish Science Journal, **3**:
16–29. doi:10.2174/1874401X01003010016.

McHenry, M.J., and Lauder, G.V. 2005. The mechanical scaling of
coasting in zebrafish (*Danio rerio*). J. Exp. Biol. **208**(12): 2289–
2301. doi:10.1242/jeb.01642. PMID:15939771.

Mchenry, M.J., Pell, C.A., and Jr, J. 1995. Mechanical control of
swimming speed: stiffness and axial wave form in undulating
fish models. J. Exp. Biol. **198**(11): 2293–2305. PMID:9320209.

McLain, D.H. 1974. Drawing contours from arbitrary data points.
Comput. J. **17**: 318–324.

Müller, U.K., and van Leeuwen, J.L. 2004. Swimming of larval
zebrafish: ontogeny of body waves and implications for locomo-
tory development. J. Exp. Biol. **207**(5): 853–868. doi:10.1242/
jeb.00821. PMID:14747416.

Müller, U.K., van den Boogaart, J.G.M., and van Leeuwen, J.L.
2008. Flow patterns of larval fish: undulatory swimming in the
intermediate flow regime. J. Exp. Biol. **211**(2): 196–205.
doi:10.1242/jeb.005629. PMID:18165247.

Osman, A.G.M., Wuertz, S., Mekkawy, I.A., Verreth, J., and
Kirschbaum, F. 2008. Early development of the African catfish
Clarias gariepinus (Burchell, 1822), focusing on the ontogeny
of selected organs. J. Appl. Ichthyology, **24**(2): 187–195.
doi:10.1111/j.1439-0426.2007.01018.x.

Osse, J.W.M. 1989. Form changes in fish larvae in relation to
changing demands of function. Neth. J. Zool. **40**(1): 362–385.
doi:10.1163/156854289X00354.

Osse, J.W.M., and van den Boogaart, J.G.M. 1999. Dynamic
morphology of fish larvae, structural implications of friction
forces in swimming, feeding and ventilation. J. Fish Biol.
55(Suppl. A): 156–174. doi:10.1111/j.1095-8649.1999.tb01053.x.

Osse, J.W.M., and van den Boogaart, J.G.M. 1995. Fish larvae, de-
velopment, allometric growth, and the aquatic environment.
ICES J. Mar. Sci. Symp. **201**: 21–34.

Osse, J.W.M., and van den Boogaart, J.G.M. 2000. Body size and
swimming types in carp larvae: effects of being small. Neth. J.
Zool. **50**(2): 233–244.

Read, D.A., Hover, F.S., and Triantafyllou, M.S. 2003. Forces on
oscillating foils for propulsion and maneuvering. J. Fluids
Struct. **17**(1): 163–183. doi:10.1016/S0889-9746(02)00115-9.

Sfakiotakis, M., Lane, D.M., and Davies, J.B.C. 1999. Review of
fish swimming modes for aquatic locomotion. IEEE J. Oceanic
Eng. **24**(2): 237–252. doi:10.1109/48.757275.

Taylor, G.K., Nudds, R.L., and Thomas, A.L.R. 2003. Flying and
swimming animals cruise at a Strouhal number tuned for high
power efficiency. Nature (London), **425**(6959): 707–711.
doi:10.1038/nature02000. PMID:14562101.

Thorsen, D.H., Cassidy, J.J., and Hale, M.E. 2004. Swimming of
larval zebrafish: fin-axis coordination and implications for func-
tion and neural control. J. Exp. Biol. **207**(24): 4175–4183.
doi:10.1242/jeb.01285. PMID:15531638.

Tytell, E.D. 2004. The hydrodynamics of eel swimming II. Effect
of swimming speed. J. Exp. Biol. **207**(19): 3265–3279. doi:10.
1242/jeb.01139. PMID:15326203.

van Raamsdonk, W., Pool, C.W., and te Kronnie, G. 1978. Differ-
entiation of muscle fiber types in the teleost *Brachydanio rerio*.
Anat. Embryol. (Berl.), **153**(2): 137–155. doi:10.1007/
BF00343370. PMID:677468.

van Raamsdonk, W., van't Veer, L., Veeken, K., Heyting, C., and
Pool, C.W. 1982. Differentiation of muscle fiber types in the tel-
eost *Brachydanio rerio*, the zebrafish. Anat. Embryol. (Berl.),
164(1): 51–62. doi:10.1007/BF00301878. PMID:7114488.

van Raamsdonk, W., Mos, W., Smit-Onel, M.J., van der Laarse,
W.J., and Fehres, R. 1983. The development of the spinal motor
column in relation to the myotomal muscle fibers in the zebra-
fish (*Brachydanio rerio*). Anat. Embryol. (Berl.), **167**(1): 125–
139. doi:10.1007/BF00304606. PMID:6881540.

Videler, J.J. 1981. Swimming movements, body structure and pro-
pulsion in cod *Gadus morhua*. Symp. Zool. Soc. Lond. **48**: 1–27.

Videler, J.J. 1993. Fish swimming. Chapman and Hall, London.

Videler, J.J., and Wardle, C.S. 1991. Fish swimming stride by
stride: speed limits and endurance. Rev. Fish Biol. Fish. **1**(1):
23–40. doi:10.1007/BF00042660.

Webb, P.W., and Weihs, D. 1986. Functional locomotor morphology
of early life history stages of fishes. Trans. Am. Fish. Soc. **115**(1):
115–127. doi:10.1577/1548-8659(1986)115<115:FLMOEL>2.0.
CO;2.

Weihs, D. 1973. The mechanism of rapid starting of slender fish.
Biorheology, **10**(3): 343–350. PMID:4772008.

Weihs, D. 1974. Energetic advantages of burst swimming of fish. J.
Theor. Biol. **48**(1): 215–229. doi:10.1016/0022-5193(74)90192-
1. PMID:4456041.

Weihs, D. 1980. Energetic significance of changes in swimming
modes during growth of larval anchovy, *Engraulis mordax*.
Fish. Bull. (Wash. D.C.), **77**: 597–604.